Supporting Information

Electrostatic trapping of polysulfides enabled by imidazolium-based ionic polymers for high-energy-density lithium-sulfur batteries

Zhibin Cheng,[a,c] Hui Pan,[a,b] Zhubing Xiao,[a] Dejian Chen,[a] Xiaoju Li[,b] and Ruihu Wang*[,a]*

[a]State Key Laboratory of Structural Chemistry, Fujian Institute of Research on the Structure of Matter, Chinese Academy of Sciences, Fuzhou, Fujian 350002, China

E-mail: ruihu@fjirsm.ac.cn

[b]Fujian Key Laboratory of Polymer Materials, College of Materials Science and Engineering, Fujian Normal University, Fuzhou, Fujian, 350007, China.

Email: xiaojuli@fjnu.edu.cn

[c]University of Chinese Academy of Sciences, Beijing, 100049, China

Experimental section

Materials: 1,3,5-Tris(bromomethyl)-2,4,6-trimethylbenzene,[S1] 1,3,5-tris(1-imidazolyl)benzene[S2] and lithium polysulfides (Li_2S_6)[S3] were prepared according to the reported literature methodes. Multiwalled carbon nanotube (CNTs, >99.9%) was purchased from Aladdin Industrial Corporation. Flake graphite was purchased from Qingdao Tianhe Graphite Corporation. Lithium sulfide was purchased from Alfa Aesar.

Structure characterization: Powder X-ray diffraction (XRD) patterns were recorded in the range of 2θ = 5-70° on a desktop X-ray diffractometer (RIGAKU-Miniflex 600) with Cu Kα radiation. Elemental analysis was performed by using an Elementar Vario MICRO Elemental analyzer. Elemental analysis was performed by using an Elementar Vario MICRO Elemental analyzer. Thermogravimetric analysis (TGA) was measured at a heating rate of 10 °C min^{-1} using a STA449 C Jupiter thermo gravimetric analyzer (NETZSCH). Scanning electron microscope (SEM) images were obtained with a JSM-6700F field-emission scan electron microscope. Transmission electron microscope (TEM) images were obtained on TECNAI G2F20. Liquid UV-Vis spectroscopic analyses were performed on a Lambda35 UV-Vis spectrophotometer

Preparation of the CNT/IP composite: The multiwall CNTs (500 mg) in sulfuric acid (98%) and nitric acid (60%) with a 3:1 ratio was heated at 80 °C for 2 h. After cooling to room temperature, the reaction was quenched with water, and the mixture was centrifuged. The remaining solid was washed with copious water until neutral pH. The post-treated CNTs (50 mg) and 1,3,5-tris(1-imidazolyl)benzene (70 mg, 0.253 mmol) in DMF (80 mL) were mixed ultrasonically for 2 h, and then 1,3,5-tris(bromomethyl)-2,4,6-trimethylbenzene (100 mg, 0.253 mmol) was added at room temperature. The resultant mixture was stirred at room temperature for 1h, and then heated at 110 °C for 12 h. The black powder was filtered,

washed with DMF and ethanol, and dried at 60°C *in vacuo* overnight to afford the CNT/IP composite.

Preparation of the N,S-codoped reduced graphene oxide (rGO): The graphene oxide (GO) was synthesized from flake graphite by a modified Hummers method. GO (500 mg) was added to the ethanol solution (80 mL) of dibenzothiazole disulfide (200 mg), followed by ultrasound for 3 h, and then transferred into a Teflon-lined autoclave. After heated at 180 ^{o}C for 12 h, rGO was obtained by filtering and washing with warm ethanol for three times.

Preparation of the rGO/S composite: The rGO/S composite was prepared using a conventional melt-diffusion method. In a typical procedure, rGO and sulfur with a mass ratio of 7:13 were ground and dispersed in CS_2 solution, and then the mixture was stirred at room temperature until CS_2 was completely evaporated. The resultant mixture was heated at 155 °C for 24 h. The rGO/S composite was collected after cooling to room temperature.

Preparation of the rGO/S+CNT/IP composite: A mixture of rGO/S and CNT/IP with the weight ratio of 3:1 was fully ground, and then dispersed in deionized water. After the mixture was stirred and ultrasonicated at room temperature for 15 min, the mixture was filtrated rapidly and dried at 60 °C for 12 h to generate the rGO/S+CNT/IP composite.

The rGO/S+CNT composite was prepared using the same procedures except that CNT/IP was replaced by CNT.

Preparation of the rGO/S+CNT/IP electrode: A mixture of rGO/S+CNT/IP, acetylene black and PVDF with the weight ratio of 8:1:1 in NMP was stirred to form homogeneous slurry. The slurry was then plastered onto aluminum foil using a doctor blade, and dried at 60 °C for 24 h in a vacuum oven. Before testing, the cathode was compacted by a roll press.

For comparison, the rGO/S+CNT electrode was prepared using the same procedures except rGO/S+CNT/IP was replaced by rGO/S+CNT.

Electrochemical Measurements: CR2025 coin cells with the rGO/S+CNT/IP and rGO/S+CNT/IP cathodes as the working electrodes, lithium foils as a counter electrode and

Celgard 2400 as a separator were assembled in a glove box filled with argon gas. The average sulfur loadings in rGO/S+CNT/IP and rGO/S+CNT were 2.1 and 2.0 mg cm^{-2}, respectively. And the cathodes contained 38.4 wt% of sulfur in the whole cathode electrode. The electrolyte was 1 M lithium bis(trifluoromethane sulfonyl)imide (LiTFSI) in a mixed solvent of 1,3-dioxolane (DOL) and 1,2-dimethoxyethane (DME) (1:1, v/v) with 1% $LiNO_3$. The electrode was cut into circular pieces with 7 mm radius and the electrolyte to sulfur ratio in a microliter of electrolyte to milligrams of sulfur is about 9.5 μL:1.0 mg. The discharge/charge measurements were conducted at a voltage interval from 1.5 to 3.0 V using a Neware battery test system (Neware Technology Co.). Cyclic voltammetry (CV) and electrochemical impedance spectroscopy (EIS) measurements were performed on CHI604E electrochemical workstation. The CV scan rate was fixed at 0.1 mV s^{-1} and EIS was measured with an applied sinusoidal excitation voltage of 5 mV in the frequency range from 100 kHz to 0.1 Hz.

Adsorption test of lithium polysulfides: All samples were dried under vacuum at 80 ºC overnight before the adsorption test. Li_2S_6 was prepared by chemical reaction between sublimed sulfur and Li_2S with a molar ratio of 5:1 in DOL/DME solution (1:1, v/v). The solution was stirred under nitrogen atmosphere at 70 ºC overnight to produce a brownish-red Li_2S_6 solution (1.0 M). The Li_2S_6 solution was then diluted to 5 mM for the polysulfide adsorption test.

The calculation for weight percentage of ImIP in CNT/IP: Weight percentage of ImIP in CNT/IP was calculated based on the N wt% in the CNT/IP. The theoretical nitrogen content in the ImIP is 14 × 6 / 674.7 × 100 wt% = 12.45 wt%. Elemental analysis show that nitrogen content in CNT/IP is 7.63 wt%. Thus, the content of ImIP in CNT/IP can be estimated as: 7.63 wt% / 12.45 wt% × 100wt% = 61.29 wt%.

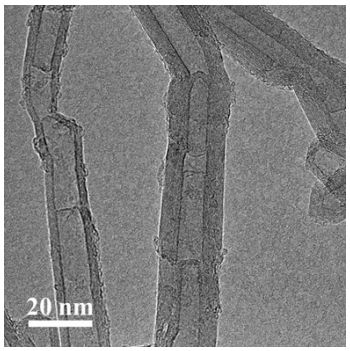

Figure S1. TEM image of CNTs.

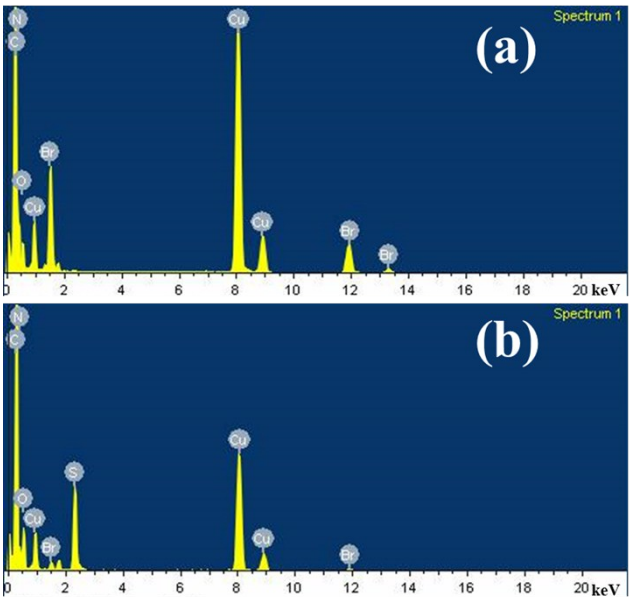

Figure S2.EDX elementary analysis of (a) CNT/IP and (b) Li_2S_6-treated CNT/IP.

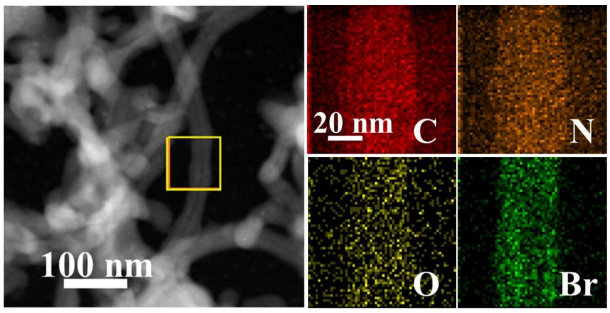

Figure S3 HAADF-STEM image and the corresponding elemental mappings of CNT/IP.

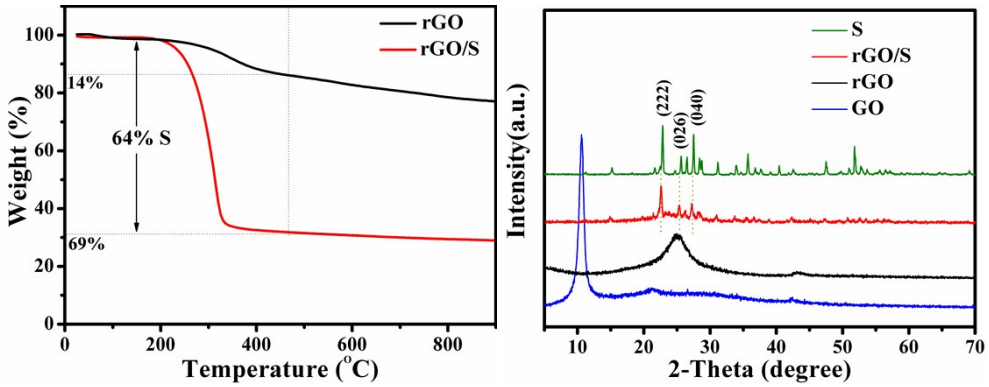

Figure S4. (a) TGA curve of rGO and rGO/S. (b) XRD patterns of S, rGO/S, rGO and GO.

The TGA curves show that rGO has weight loss of 14 wt% in the temperature range from 200 to 470 °C, so the total weight loss of 69 wt% for rGO/S in the range from 200 to 470 °C contains the fully evaporated sulfur (m_s) and the weight loss of rGO [($m_{rGO/S}$-m_s) × 14 wt%]. Thus, [($m_{rGO/S}$-m_s) × 14 wt%] + (m_s) = 69 wt% × $m_{rGO/S}$. Finally, the content of sulfur in rGO/S can be estimated as:

S wt% = m_s / $m_{rGO/S}$ × 100 wt% = (69 wt% - 14 wt%) / (100 wt% - 14 wt%) × 100 wt% ≈ 64 wt%.

where $m_{rGO/S}$ represents the total mass of rGO/S. It should be mentioned that the doped sulfur in as-prepared rGO can be neglected. Elemental analysis was performed to reconfirm the sulfur content of the sample, sulfur loading in rGO/S was 64.39 wt%, which are consistent with the TGA result.

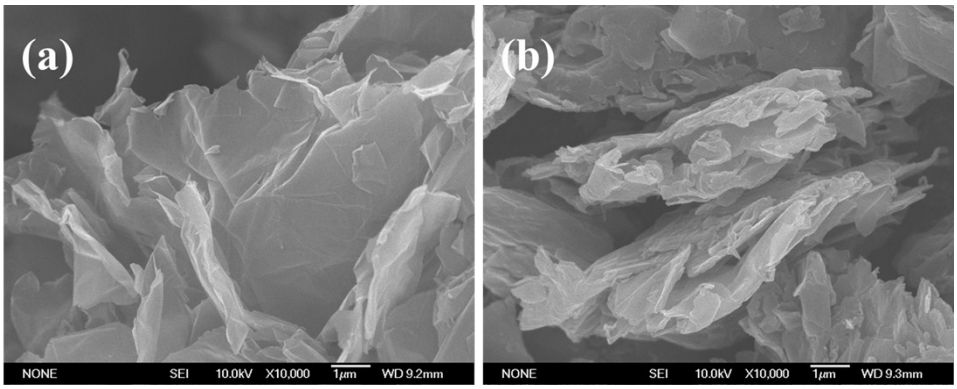

Figure S5. SEM images of (a) rGO and (b) rGO/S.

N,S-codoped reduced graphene oxide (rGO) was readily prepared through solvothermal treatment of graphene oxide and dibenzothiazole disulfide. Elementary analysis shows the

nitrogen and sulfur contents in as-prepared rGO are 0.73% and 2.67%, respectively. rGO/S was prepared through a conventional sulfur melt-diffusion method. Sulfur content in the rGO/S composite is 64 wt% as determined by thermogravimetric analysis (TGA) (Figure S4a). The typical reflection peaks of element sulfur can be clearly identified in powder X-ray diffractometer (XRD) patterns of rGO/S (Figure S4b), which can be indexed as Fddd orthorhombic structure of crystalline sulfur. SEM images show that rGO/S consists of sandwich-structured nanosheets, sulfur particles reside on the two surface of the rGO nanosheets (Figure S5). All of these would consequently lead to the easy dissolution of lithium polysulfides in the charge-discharge electrochemical process and inevitably compromise the cycling stability of the sulfur cathodes. Compared with rGO (Figure S5), an obvious increment of the sheet thickness is observed in rGO /S, and there are no distinguishable bulk sulfur particles or their agglomeration.

In order to evaluate the electrochemical stability of CNT/IP composite, the CNT/IP composite, CNT and binder were mixed at a weight ratio of 80:10:10 in N-methyl-2-pyrrolidone (NMP) to form homogeneous slurry under magnetic stirring. After that, the slurry was then plastered onto aluminum foil using a doctor blade, and dried at 60 °C for 24 h in a vacuum oven. Cyclic voltammograms of the obtained electrode between 1.5 and 3 V (vs. Li^+/Li) were recorded at a potential scanning rate of 0.1 mV s^{-1}. As shown in Figure 2k, there is no redox peak from both of these two electrodes within a potential range of 1.75 to 3.0 V (vs. Li/Li^+), indicating that the CNT/IP composite will not react with the Li^+ during the electrochemical reaction. In addition, there is a reduction peak in both of the curves below 1.75 V (vs. Li/Li^+), and the current peak is gradually decreased with continuous cycles. This is attributed to the reaction between the $LiNO_3$ and the metal Li anode.

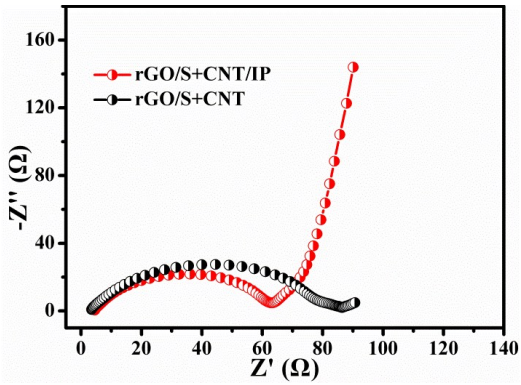

Figure S6. EIS spectra of rGO/S+CNT/IP and rGO/S+CNT.

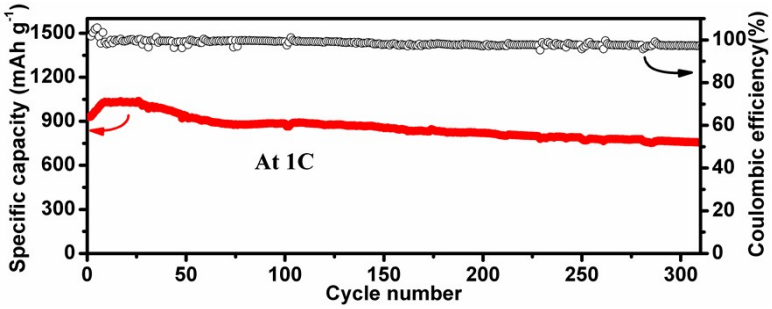

Figure S7. Cycling performance of rGO/S+CNT/IP at 1 C;

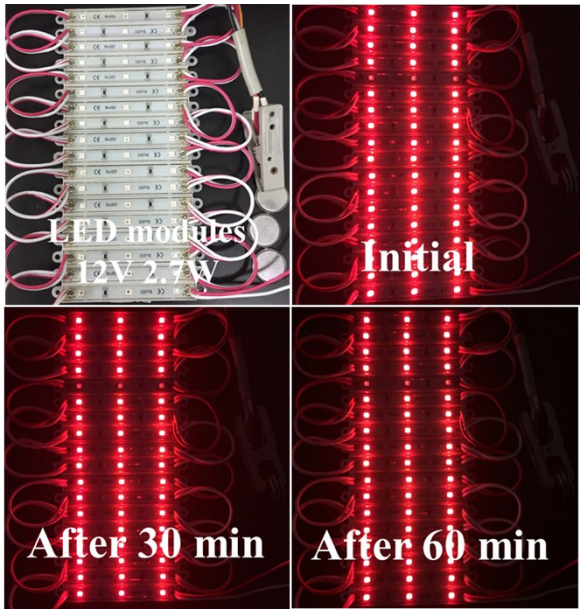

Figure S8. Digital photographs of 54 yellow indicators composed of 2835 LED modules powered by three rGO/S+CNT/IP batteries in series.

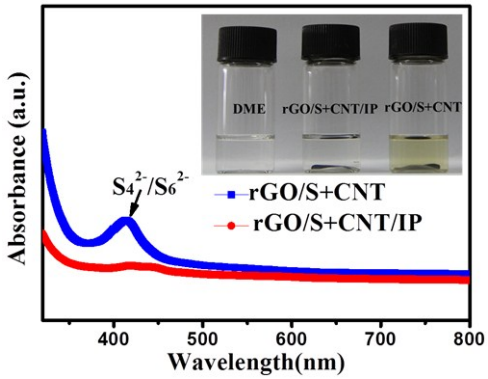

Figure S9 Photos of color change for the solution of cycled rGO/S+CNT and rGO/S+CNT/IP cathode pieces in DME for 12 h (inset) and the corresponding UV-vis spectra.

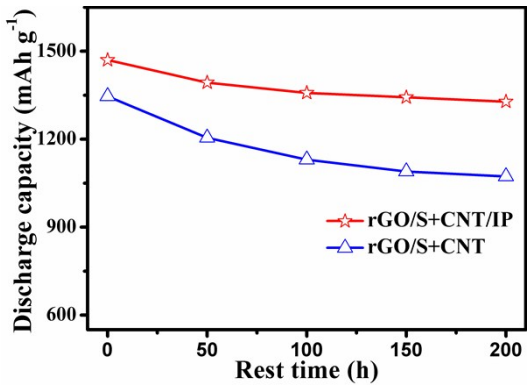

Figure S10 Self-discharge behavior of rGO/S+CNT/IP and rGO/S+CNT cathodes. The cathodes were tested with a current density of 0.05 C.

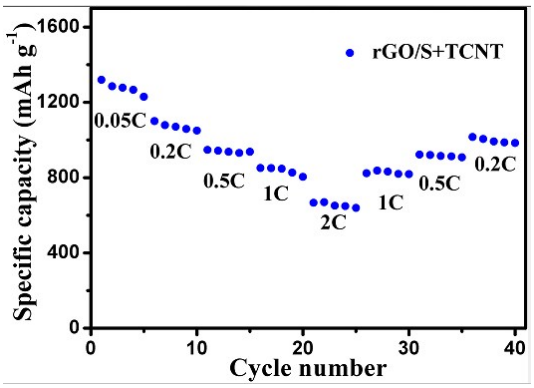

Figure S11 Rate performance for rGO/S+TCNT cathode.

The rGO/S+TCNT composite cathode with ~2.0 mg cm^{-2} sulfur loading was prepared using the same procedures for preparation rGO/S+CNT cathode except that pristine CNT was replaced by acid-pretreated CNT. The rate performance for rGO/S+TCNT, rGO/S+CNT, and rGO/S+CNT/IP were shown in Figure 4c and S11. Obviously, the rGO/S+TCNT cathode

exhibited similar rate performance to rGO/S+CNT but much lower than rGO/S+CNT/IP, which confirms that pretreated for pristine carbon nanotube could not display significantly enhanced electrochemical performance for the whole cathode.

Table S1. Results of this work compared to the values of reported slurry-coated electrode materials.

Cathode materials	Sulfur loading (mg cm^{-2})	Current rate (C)[a)]	The first discharge capacity (mA h g^{-1})	Reversible discharge capacity (mA h g^{-1})	Total cycle number	Reference
HGC/S	1.0	0.2	1250	952	60	S4
CH@LDH	3	0.1	1014	653	100	S5
HCSs/S-LBL	0.87-1.1	0.6	~850	575	200	S6
C/S+BTO	2.4	0.2	1143	835	100	S7
N-PCB/S	2.5-2.7	0.1/1	1223/<900	1010/746	100	S8
TiO@C-HS	1.5 4	0.2 0.05	1285 886	750 821	500 50	S9
S@rGO-HCS	0.8-1.0	0.5	901	712	400	S10
S-CNTs@CNT	2	0.1	1633	1193	100	S11
S@SCNMM	<1.0	1	-	860	100	S12
CPS-70	1.2	0.5	~950	750	300	S13
S/GN-CNT	1.3-1.6	0.1	1373.8	836.5	200	S14
S/N-HPCB	1.1-1.5	1	1192	706	400	S15
CNT/S+G@CB	4.2	0.1	900	800	90	S16
S-a-PCNT	2.2	0.2	1256	917	300	S17
CNT-nest-S	2.5-3	0.1	937	800	>80	S18
SF-CTF-1s	0.7	0.6	637.3	520	300	S19
S@M-MGCSs	3.2	0.2	994	826	100	S20
TiC@G/S	3.5	0.2	1032	670	100	S21
S@CNTs/Co_3S_4	3.5	0.2	1012	820	150	S22
rGO/S+CNT/IP	**2.1** **4.2**	**0.2/1** **0.15**	**1180/935** **1131**	**1045/751** **914**	**120/310** **120**	This work

[a)] 1C=1675 mA g^{-1}

Supplementray Reference

S1. G. Periyasami, R. Rajesh, N. Arumugam, R. Raghunathan, S. Ganesan and P. Maruthamuthu, *J. Mater. Chem. A*, 2013, **1**, 14666-14674.

S2. J. Fan, L. Gan, H. Kawaguchi, W. Y. Sun, K. B. Yu and W. X. Tang, *Chem. Eur. J.* , 2003, **9**, 3965-3973.

S3. G. Zhou, H. Tian, Y. Jin, X. Tao, B. Liu, R. Zhang, Z. W. Seh, D. Zhuo, Y. Liu, J. Sun, J. Zhao, C. Zu, D. S. Wu, Q. Zhang and Y. Cui, *Proc. Natl. Acad. Sci.*, 2017, **114**, 840-845.

S4. J. Jia, K. Wang, X. Zhang, X. Sun, H. Zhao and Y. Ma, *Chem. Mater.*, 2016, **28**, 7864-7871.

S5. J. Zhang, H. Hu, Z. Li and X. W. Lou, *Angew. Chem., Int. Ed.*, 2016, **55**, 3982-3986.

S6. F. Wu, J. Li, Y. Su, J. Wang, W. Yang, N. Li, L. Chen, S. Chen, R. Chen and L. Bao, *Nano Lett.*, 2016, **16**, 5488-5494.

S7. K. Xie, Y. You, K. Yuan, W. Lu, K. Zhang, F. Xu, M. Ye, S. Ke, C. Shen, X. Zeng, X. Fan and B. Wei, *Adv. Mater.*, 2017, **29**, 1604724.

S8. F. Zeng, K. Yuan, A. Wang, W. Wang, Z. Jin and Y. S. Yang, *J. Mater. Chem. A*, 2017, **5**, 5559-5567.

S9. Z. Li, J. Zhang, B. Guan, D. Wang, L. M. Liu and X. W. Lou, *Nat. Commun.*, 2016, **7**, 13065.

S10. S. Liu, K. Xie, Z. Chen, Y. Li, X. Hong, J. Xu, L. Zhou, J. Yuan and C. Zheng, *J. Mater. Chem. A*, 2015, **3**, 11395-11402.

S11. F. Jin, S. Xiao, L. Lu and Y. Wang, *Nano Lett.*, 2016, **16**, 440-447.

S12. X. Chen, Z. Xiao, X. Ning, Z. Liu, Z. Yang, C. Zou, S. Wang, X. Chen, Y. Chen and S. Huang, *Adv. Energy Mater.*, 2014, **4**, 1301988.

S13. L. Ma, H. L. Zhuang, S. Wei, K. E. Hendrickson, M. S. Kim, G. Cohn, R. G. Hennig and L. A. Archer, *ACS Nano*, 2016, **10**, 1050-1059.

S14. Z. Zhang, L. L. Kong, S. Liu, G. R. Li and X. P. Gao, *Adv. Energy Mater.*, 2017, **7**, 1602543.

S15. F. Pei, T. An, J. Zang, X. Zhao, X. Fang, M. Zheng, Q. Dong and N. Zheng, *Adv. Energy Mater.*, 2016, **6**, 1502539.

S16. J. Xie, H. J. Peng, J. Q. Huang, W. T. Xu, X. Chen and Q. Zhang, *Angew. Chem., Int. Ed.*, 2017, **56**, 16223-16227

S17. J. S. Lee, J. Jun, J. Jang and A. Manthiram, *Small*, 2017, **13**, 1602984.

S18. G. Ai, Y. Dai, W. Mao, H. Zhao, Y. Fu, X. Song, Y. En, V. S. Battaglia, V. Srinivasan and G. Liu, *Nano Lett.*, 2016, **16**, 5365-5372.

S19. S. H. Je, H. J. Kim, J. Kim, J. W. Choi and A. Coskun, *Adv. Funct. Mater.*, 2017, **7**, 1703947.

S20. J. Zheng, G. Guo, H. Li, L. Wang, B. Wang, H. Yu, Y. Yan, D. Yang and A. Dong, *ACS Energy Lett.*, 2017, **2**, 1105-1114.

S21. H. J. Peng, G. Zhang, X. Chen, Z. W. Zhang, W. T. Xu, J. Q. Huang and Q. Zhang, *Angew. Chem., Int. Ed.*, 2016, **55**, 12990-12995.

S22. T. Chen, Z. Zhang, B. Cheng, R. Chen, Y. Hu, L. Ma, G. Zhu, J. Liu and Z. Jin, *J. Am. Chem. Soc.*, 2017, **139**, 12710-12715.